Probabilistic Analysis of Small-signal Stability of Large-scale Power Systems as Affected by Penetration of Wind Generation

Probabilistic Analysis of Small-signal Stability of Large-scale Power Systems as Affected by Penetration of Wind Generation

S. Q. Bu, *Student Member, IEEE,* W. Du, H. F. Wang, *Senior Member, IEEE,* Z. Chen, L. Y. Xiao and H. F. Li

***Abstract*—This paper proposes a method of probabilistic analysis to investigate the impact of stochastic uncertainty of grid-connected wind generation on power system small-signal stability. The proposed method is "analytical" in contrast to the numerical method of Monte Carlo simulation which relies on large number of random computations. It can directly calculate the probabilistic density function (PDF) of critical eigenvalues of a large-scale power system from the PDF of grid-connected multiple sources of wind power generation, thus to determine the probabilistic small-signal stability of the power system as affected by the wind generation. In the paper, an example of 16-machine power system with 3 grid-connected wind farms is used to demonstrate the application of the proposed method. The results of probabilistic stability analysis of the example power system are confirmed by the Monte Carlo simulation. It is shown that the stochastic variation of grid-connected wind generation can cause the system to lose stability even though the system is stable deterministically. The higher the level of wind penetration is, the more the probability that the system becomes unstable could be. Hence indeed penetration of stochastically variable wind generation threats stable operation of power systems as far as system small-signal stability is concerned.**

***Index Terms*—Correlations, Gram-Charlier expansion, Monte Carlo simulation, probabilistic analysis, probabilistic density function (PDF), power system small-signal stability, wind power generation.**

I. Introduction

GRID-connected wind power sources have been increasingly brought into the conventional power systems recently. Their grid connection may significantly affect power system dynamics and operational characteristics, including small-signal stability. There has been a great effort in investigating the impact of increasing penetration of wind generation on power system small-signal stability recently [1]-[6]. Though work presented in [1]-[6] are the results of case studies, it has clearly indicated that the grid-connected wind generation affects power system small-signal stability, sometimes detrimentally [1]-[6]. Therefore, it is an essentially important work to examine carefully the effect of grid-connected wind generation on power system small-signal stability. On the other hand, the generation capability of wind power sources relies on the conditions of natural environment, such as wind speed. Their grid-connection introduces significant stochastic fluctuation of generation which could be potentially spatial dependent. The impact of the generation uncertainty caused by the stochastically variable wind sources on power system small-signal stability is an issue that has neither been encountered by power transmission with conventional power generation and nor considered by the deterministic analysis in [1]-[6].

The first application of probabilistic analysis in power systems was by Borkowska (1974) in [7] for the power system load flow study (PLF), then further developed by Allan in [8] and [9]. The probabilistic analysis was firstly introduced into studying power system small-signal stability by Burchett and Heydt (1978) in [10]. Generalized tetrachoric series was used in [10] to determine the stochastic distribution density of system critical eigenvalues, hence the probability of the small-signal stability of the power system. In [10] the influence of uncertainty in system parameters from several sources subject to the multivariate normal distribution was considered. This analytical method was later developed to accommodate random variables with any type of distribution by using a moment approach in [11]. A series of work later in [12] and [13] has further improved the various aspects of the analytical methods of power system probabilistic small-signal stability, including probabilistic eigenvalue sensitivity analysis for the design of power system stabilizers in [14]-[16]. Among various methods of probabilistic analysis, the Gram-Charlier expansion based (or named cumulant-based) method of probabilistic analysis has been widely used in many applications of stochastic static analysis of power systems in [17]-[22]. The method can be used to approximate any type of distributions and is capable of handling large-scale power systems with high efficiency.

Non-analytical method to determine power system probabilistic stability is the Monte Carlo simulation [23]. It is successfully employed in [24] to study the effect of uncertainty of grid-connected wind generation on power system small-signal stability. The Monte Carlo simulation is to generate a large number of random computational scenarios according to the distribution density of the stochastic sources, such as wind. Accumulation of computational results of deterministic power system small-signal stability (the critical eigenvalues) from all the scenarios forms the distribution density of the critical eigenvalues, hence to determine the power system probabilistic stability. Obviously, though the Monte Carlo simulation can provide accurate results, it is a method of extremely time consuming. Therefore, it has been well accepted that the

Mr. S. Q. Bu, Dr. W. Du (corresponding author) and Prof. H. F. Wang are with the School of Electronics, Electrical Engineering and Computer Science, the Queen's University of Belfast, Belfast, BT7 1NN, UK.

Dr. Z Chen (Dr. W. Du was) is with the Southeast University, China. Prof. L Y Xiao is with the Institute of Electrical Engineering, the CAS, China. Dr. H. F. Li is with the Jiangsu Power Company, China.

analytical method of probabilistic analysis is more applicable, especially for the study of probabilistic stability of large-scale power systems. The Monte Carlo simulation can be used as a way to evaluate and confirm the correctness of probabilistic analysis.

This paper presents the probabilistic analysis of power system small-signal stability considering the stochastic uncertainty introduced by multiple grid-connected wind power sources and their spatial correlations. The Gram-Charlier expansion based method is employed to derive the probabilistic density function (PDF) of system critical eigenvalues from the well-known Weibull distribution of wind speed. The method of probabilistic analysis presented in the paper can determine the probabilistic small-signal stability of power systems penetrated by multiple wind power sources by just performing the step-by-step computation proposed once. Hence it successfully avoids the complex convolution calculation and high computational burden of the Monte Carlo simulation. The paper is organized as follows. In Section II, a simple case without considering the spatial correlations of grid-connected wind generation is given in order to give a clear presentation. On the basis of Section II, the case of taking account of the correlations between different wind power sources is further examined in Section III. The Gram-Charlier expansion based method is modified to accommodate the more realistic case that the grid-connected wind generation could be spatially correlated. In Section IV, an example of 16-machine 5-area power system with 3 grid-connected wind power sources is given. The Monte Carlo simulation is used to confirm the correctness and accuracy of the method proposed. Results of probabilistic stability analysis of the example power system demonstrate that the stochastic variation of grid-connected wind generation affects the small-signal stability of the power system. Probabilistic stability changes significantly with the variation of level of wind penetration.

II. Probabilistic Analysis of Small-signal Stability of Power Systems with Independent Grid-connected Multiple Wind Power Sources

A. Distribution function of wind power generation [25]

Eq. (1) is the Weibull (or normal skew) distribution, which is considered to be one of the most applicable descriptions of stochastic fluctuation of wind power generation. In (1), P_{wi} is the active power supplied by the i^{th} wind generation source (wind farm) connected to a multi-machine power system, $f_{pi}(\cdot)$ is the PDF of the wind power, v_{ci} the cut-in wind speed, v_{ri} the rated wind speed, v_{fi} the furling wind speed, $F_{si}(\cdot)$ the CDF of Weibull distribution of wind speed, $\delta(P_{wi})$ the impulse function, and P_{ri} the rated wind power.

$$f_{pi}(P_{wi}) = \begin{cases} \big[1-(F_{si}(v_{fi})-F_{si}(v_{ci}))\big]\delta(P_{wi}), \\ \qquad\qquad \text{for} \quad P_{wi}=0 \\ \dfrac{b_i}{d_i}\Big(\dfrac{P_{wi}-h_i}{d_i}\Big)^{b_i-1} exp\Big[-\Big(\dfrac{P_{wi}-h_i}{d_i}\Big)^{b_i}\Big], \\ \qquad\qquad \text{for} \quad 0<P_{wi}<P_{ri} \\ \big[F_{si}(v_{fi})-F_{si}(v_{ri})\big]\delta(P_{wi}-P_{ri}), \\ \qquad\qquad \text{for} \quad P_{wi}=P_{ri} \\ 0, \qquad \text{for} \quad P_{wi}<0 \text{ or } P_{wi}>P_{ri} \end{cases} \tag{1}$$

Parameters in (1) are given by the following equations

$$\begin{aligned} &b_i = \Big(\frac{\sigma_i}{\mu_i}\Big)^{-1.086}, d_i = \frac{P_{ri}\mu_i}{(v_{ri}-v_{ci})\Gamma(1+1/b_i)} \\ &h_i = -\frac{P_{ri}v_{ci}}{v_{ri}-v_{ci}} \end{aligned} \tag{2}$$

where $\Gamma(\cdot)$ is a Γ function, μ_i and σ_i are the mean and standard deviation of wind speed respectively.

B. Moments and cumulants of wind power generation

The wind power variation is defined to be $\Delta P_{wi} = P_{wi} - P_{w0i}$, where P_{w0i} is the deterministic wind power generation. According to the probability theory, the n^{th} moment $\alpha^{(n)}_{\Delta P_{wi}}$ of the wind power variation, ΔP_{wi}, can be computed from (1) as follows

$$\begin{aligned} \alpha^{(n)}_{\Delta P_{wi}} &= \int_{-P_{w0i}}^{P_{ri}-P_{w0i}} x^n dF_{pi}(x) = \int_{-P_{w0i}}^{P_{ri}-P_{w0i}} x^n f_{pi}(x)dx \\ &= \big[1-(F_{si}(v_{fi})-F_{si}(v_{ci}))\big](-P_{w0i})^n \\ &+ \big[F_{si}(v_{fi})-F_{si}(v_{ri})\big](P_{ri}-P_{w0i})^n \\ &+ \sum_{k=0}^{n} C_n^k (d_i)^k (h_i - P_{w0i})^{n-k} \int_{(-\frac{h_i}{d_i})^{b_i}}^{(\frac{P_{ri}-h_i}{d_i})^{b_i}} \tau^{\frac{k}{b_i}} e^{-\tau} d\tau \end{aligned} \tag{3}$$

where $C_n^k = \frac{n!}{k!(n-k)!}$ and $\int_{(-\frac{h_i}{d_i})^{b_i}}^{(\frac{P_{ri}-h_i}{d_i})^{b_i}} \tau^{\frac{k}{b_i}} e^{-\tau} d\tau$ is an incomplete Γ function. Appendix A gives details of derivation of (3).

The n^{th} order cumulant, $\gamma^{(n)}_{\Delta P_{wi}}$, also known as the semi-invariant, is the polynomial in $\alpha^{(1)}_{\Delta P_{wi}}, \alpha^{(2)}_{\Delta P_{wi}}, \cdots \alpha^{(n)}_{\Delta P_{wi}}$, for example from [26] and [27]

$$\begin{aligned} &\gamma^{(1)}_{\Delta P_{wi}} = \alpha^{(1)}_{\Delta P_{wi}} \\ &\gamma^{(2)}_{\Delta P_{wi}} = \alpha^{(2)}_{\Delta P_{wi}} - (\alpha^{(1)}_{\Delta P_{wi}})^2 \\ &\gamma^{(3)}_{\Delta P_{wi}} = \alpha^{(3)}_{\Delta P_{wi}} - 3\alpha^{(1)}_{\Delta P_{wi}}\alpha^{(2)}_{\Delta P_{wi}} + 2(\alpha^{(1)}_{\Delta P_{wi}})^3 \\ &\cdots\cdots\cdots \end{aligned} \tag{4}$$

Hence by using (4), the n^{th} order cumulant, $\gamma^{(n)}_{\Delta P_{wi}}$, can be computed from the various-order moments.

C. Cumulants and central moments of stochastic variation of critical eigenvalue

According to the probability theory in [26] and [27], if the relationship between a random variable ρ and m other independent random variables $\eta_j, j = 1, 2, \cdots m$ is linear, that is $\rho = a_1\eta_1 + a_2\eta_2 + \cdots + a_m\eta_m$, their n^{th} order cumulants satisfy the following equation

$$\gamma_\rho^{(n)} = a_1^n\gamma_{\eta_1}^{(n)} + a_2^n\gamma_{\eta_2}^{(n)} + \cdots + a_m^n\gamma_{\eta_m}^{(n)} \tag{5}$$

If there are m grid-connected wind generation sources (wind farms) in the multi-machine power system and $\lambda_k = \xi_k + j\omega_k$ is the k^{th} eigenvalue (critical eigenvalue) of the power system, the following relationship between the critical eigenvalue and the wind power generation can be established for power system small-signal stability analysis

$$\begin{aligned}\Delta\lambda_k = \Delta\xi_k + j\Delta\omega_k &= \sum_{i=1}^{m}[(\partial\lambda_k/\partial P_{wi})\Delta P_{wi}] \\ &= \sum_{i=1}^{m}\Big[\big[\mathrm{Re}(\partial\lambda_k/\partial P_{wi})\big]\Delta P_{wi} + j\big[\mathrm{Im}(\partial\lambda_k/\partial P_{wi})\big]\Delta P_{wi}\Big]\end{aligned} \tag{6}$$

where $\mathrm{Re}(\cdot)$ and $\mathrm{Im}(\cdot)$ denote the real and imaginary part of a complex variable respectively. The sensitivity of the critical eigenvalue with respect to m wind power sources at an equilibrium point in (6) can be computed conveniently in a numerical way in [28] given by the following equation

$$\frac{\partial\lambda_k}{\partial P_{wi}} = \frac{\lambda_k(P_{wi} + \Delta P_{wi}) - \lambda_k(P_{wi})}{\Delta P_{wi}}, i = 1, 2, \cdots m \tag{7}$$

The assumption of linearity is implied in deriving (6). For small-signal stability analysis, linearized model of power systems is used and the nonlinearities are not considered [29]. Hence, the assumption of linearity in (6) is tenable.

From (5) and (6) it can have

$$\gamma_{\Delta\xi_k}^{(n)} = \sum_{i=1}^{m}\left\{\left[\mathrm{Re}(\frac{\partial\lambda_k}{\partial P_{wi}})\right]^n\gamma_{\Delta P_{wi}}^{(n)}\right\} \tag{8}$$

where $\gamma_{\Delta\xi_k}^{(n)}$ is the n^{th} order cumulant of the stochastic variation of the real part of the critical eigenvalue, $\Delta\xi_k$. The mean of $\Delta\xi_k$ is $\mu_{\Delta\xi_k} = \gamma_{\Delta\xi_k}^{(1)}$. It is noted that (8) is derived under the assumption that all the wind power sources are independent. In practice this is true if wind farms locate far away to each other geographically. The spatial correlations between different wind farms will be considered in Section III.

The n^{th} order central moment, $\beta_{\Delta\xi_k}^{(n)}$, of $\Delta\xi_k$ is calculated from its cumulants by using the following equations in [26] and [27]

$$\begin{aligned}&\beta_{\Delta\xi_k}^{(1)} = 0 \\ &\beta_{\Delta\xi_k}^{(2)} = \gamma_{\Delta\xi_k}^{(2)} = \sigma_{\Delta\xi_k}^2 \\ &\beta_{\Delta\xi_k}^{(3)} = \gamma_{\Delta\xi_k}^{(3)} \\ &\beta_{\Delta\xi_k}^{(4)} = \gamma_{\Delta\xi_k}^{(4)} + 3(\gamma_{\Delta\xi_k}^{(2)})^2 \\ &\cdots\cdots\cdots\end{aligned} \tag{9}$$

where $\sigma_{\Delta\xi_k}$ is the standard deviation of $\Delta\xi_k$.

D. Gram-Charlier expansion

From the cumulants and central moments of $\Delta\xi_k$, the CDF of the standardized $\Delta\xi_k$, $\Delta\bar{\xi}_k = \frac{\Delta\xi_k - \mu_{\Delta\xi_k}}{\sigma_{\Delta\xi_k}}$, can be obtained by using the following well-known Gram-Charlier expansion

$$F_{\Delta\bar{\xi}_k}(x) = g_0\Phi(x) + \frac{g_1}{1!}\Phi^{'}(x) + \frac{g_2}{2!}\Phi^{''}(x) + \frac{g_3}{3!}\Phi^{'''}(x) + \cdots \tag{10}$$

where $F_{\Delta\bar{\xi}_k}(x)$ is the CDF of $\Delta\bar{\xi}_k$, $\Phi(x)$ the CDF of standard normal distribution respectively and the prime symbol denotes various-order derivatives of $\Phi(x)$. Coefficients in the Gram-Charlier expansion of (10) are the polynomial in the central moments of $\Delta\xi_k$ as given by [26] and [27] as follows

$$\begin{aligned}&g_0 = 1 \\ &g_1 = g_2 = 0 \\ &g_3 = -\frac{\beta_{\Delta\xi_k}^{(3)}}{\sigma_{\Delta\xi_k}^3} \\ &g_4 = \frac{\beta_{\Delta\xi_k}^{(4)}}{\sigma_{\Delta\xi_k}^4} - 3 \\ &\cdots\cdots\cdots\end{aligned} \tag{11}$$

E. CDF and PDF of real part of critical eigenvalue

Obviously, the CDF of $\Delta\xi_k$ can easily be obtained from that of $\Delta\bar{\xi}_k$ to be

$$F_{\Delta\xi_k}(x) = F_{\Delta\bar{\xi}_k}(\frac{x - \Delta\mu_{\Delta\xi_k}}{\sigma_{\Delta\xi_k}}) \tag{12}$$

Because $\Delta\xi_k = \xi_k - \xi_{k0}$ (ξ_{k0} is the deterministic value of the real part of λ_k), the CDF of ξ_k can be obtained to be

$$F_{\xi_k}(x) = F_{\Delta\xi_k}(x - \xi_{k0}) \tag{13}$$

The PDF $f_{\xi_k}(x)$ is the derivative of the CDF of ξ_k obtained in (13).

The wind power distribution is not continuous as given by (1)[25], and thus $f_{\xi_k}(x) \neq 0$ only exists over a certain interval of ξ_k, i.e., $\left[\xi_{kl}, \xi_{kr}\right]$. The CDF and PDF given by (13) is for ξ_k within $\left[\xi_{kl}, \xi_{kr}\right]$ and their value at the left end ($\xi_k = \xi_{kl}$) and right end ($\xi_k = \xi_{kr}$) of the interval needs to be calculated separately. Hence (13) needs to be modified. This modification is carried out by dividing the wind generation sources into two groups firstly. Group A is of positive $\mathrm{Re}(\partial\lambda_k/\partial P_{wi})$ and group B is of negative $\mathrm{Re}(\partial\lambda_k/\partial P_{wi})$. In deterministic eigenvalue analysis, ξ_k is calculated as ξ_{kl}, when the wind

generation sources in group A is at the cut-in wind power (i.e., $P_{wi}=0, i\in$ A) and in group B is at the furling wind power (i.e., $P_{wi}=P_{ri}, i\in$ B). ξ_{kr} is calculated similarly but when the wind generation sources in group A is at the furling wind power and group B the cut-in wind power. The modified CDF and PDF are

$$f_{\xi_k}(x)=\begin{cases}\prod\limits_{i_1\in \text{A},i_2\in \text{B}}\big[1-(F_{si_1}(v_{fi_1})-F_{si_1}(v_{ci_1}))\big] \\ \qquad\times\big[F_{si_2}(v_{fi_2})-F_{si_2}(v_{ri_2})\big]\delta(x-\xi_{kl}), \\ \qquad\qquad\qquad\text{for}\quad x=\xi_{kl} \\ \text{derivative of (13)}, \quad \text{for}\quad \xi_{kl}<x<\xi_{kr} \\ \prod\limits_{i_1\in \text{B},i_2\in \text{A}}\big[1-(F_{si_1}(v_{fi_1})-F_{si_1}(v_{ci_1}))\big] \\ \qquad\times\big[F_{si_2}(v_{fi_2})-F_{si_2}(v_{ri_2})\big]\delta(x-\xi_{kr}), \\ \qquad\qquad\qquad\text{for}\quad x=\xi_{kr} \\ 0, \quad \text{for}\quad x<\xi_{kl}\text{ or }x>\xi_{kr}\end{cases}$$

$$F_{\xi_k}(x)=\begin{cases}0, & \text{for}\quad x\le\xi_{kl}\\ (13), & \text{for}\quad \xi_{kl}<x<\xi_{kr}\\ 1, & \text{for}\quad x\ge\xi_{kr}\end{cases} \tag{14}$$

Finally the probability of the small-signal stability of the power system with m grid-connected wind power sources, as far as the k^{th} eigenvalue (critical eigenvalue) is concerned, can be defined and computed to be

$$P(\xi_k<0)=F_{\xi_k}(0)=\int_{-\infty}^{0}f_{\xi_k}(x)dx \tag{15}$$

where $F_{\xi_k}(x)$ and $f_{\xi_k}(x)$ are the CDF and PDF of ξ_k respectively.

III. Consideration of Spatial Correlations between Wind Power Sources

A. Spatial correlations of wind generation

As it is explained in [30], the correlation between two wind power sources is closely related to their geographical distance. Two locations over 1200km have a correlation coefficient close to 0, whilst very close locations (less than 100km) have a correlation coefficient close to 1. This can be used to approximately estimate their correlation coefficient ρ_{ij} and thus to establish the correlation coefficient matrix $\big[\rho_{ij}\big]_{m\times m}$ for m grid-connected wind power sources [30].

If there are sufficient wind speed data available, the correlations between pairs of wind speed can be calculated to be

$$\rho_{ij}=\frac{Cov(v_i,v_j)}{\sigma_{v_i}\sigma_{v_j}} \tag{16}$$

where v_i and v_j are wind speed random variables corresponding to two wind power source locations, $Cov(v_i,v_j)$ represents the covariance of the speed v_i and v_j, and σ_{v_i} and σ_{v_j} are the standard deviations of the speeds.

For each wind speed random variable, v_i or v_j, a wind speed sample series can be generated correspondingly. Each wind speed sample series should satisfy the Weibull distribution and contain the spatial correlation. There are several methods available to generate the eligible wind speed sample series, such as the normal transformation method in [31] and [32] and the Copulas in [33].

With the wind speed sample series available, the wind power sample series with correlations (i.e., $\big[P_{wi}\big]_{N_s\times 1}$) can be generated by employing the power-wind speed curve of each wind power sources described in [25]. The wind power variation sample series $\big[\Delta P_{wi}\big]_{N_s\times 1}$ can be obtained to be

$$\big[\Delta P_{wi}\big]_{N_s\times 1}=\big[P_{wi}\big]_{N_s\times 1}-\big[P_{w0i}\big]_{N_s\times 1}, i=1,2,\cdots m \tag{17}$$

where N_s is the size of each wind power sample series and $\big[P_{w0i}\big]_{N_s\times 1}$ is a vector with all the samples equal to the deterministic value P_{w0i}.

B. Modification of (8) to consider the wind correlations

When the correlation of the different wind power sources is considered, (8) is modified to calculate the n^{th} order cross cumulant of $\Delta\xi_k$ to be

$$\gamma^{(n)}_{\Delta\xi_k}=\sum_{i_1=1}^{m}\sum_{i_2=1}^{m}\cdots\sum_{i_n=1}^{m}\Big[\underbrace{\text{Re}(\frac{\partial\lambda_k}{\partial P_{wi_1}})\times\cdots\times\text{Re}(\frac{\partial\lambda_k}{\partial P_{wi_n}})}_{n}\gamma^{(n)}_{\Delta P_{wi_1\cdots i_n}}\Big] \tag{18}$$

where $\gamma^{(n)}_{\Delta P_{wi_1\cdots i_n}}$ denotes the n^{th} order cross cumulants of the multiple wind power variations. For independent wind power sources, $i_1=i_2=\cdots=i_n=i$. The cumulant $\gamma^{(n)}_{\Delta P_{wi_1\cdots i_n}}$ is equal to $\gamma^{(n)}_{\Delta P_{wi}}$ and (18) becomes (8).

Normally the higher order cross cumulants of $\Delta\xi_k$ have less impact on the accuracy of the CDF and PDF curve of ξ_k. Hence it is only needed to calculate the first several order cross cumulants of $\Delta\xi_k$ by using (18) to include the correlation. The cumulants of the rest with higher orders can still be calculated by (8) so as to reduce the computation cost. The 1^{st} order cross cumulant of wind power variation is still $\gamma^{(1)}_{\Delta P_{wi}}$. Their 2^{nd} and 3^{rd} order cross cumulants can be easily calculated from the following equations given by [26] and [27]

$$\begin{aligned}\gamma^{(2)}_{\Delta P_{wi_1i_2}}&=\beta^{(2)}_{\Delta P_{wi_1i_2}}\\ &=E\big[(\Delta P_{wi_1}-\mu_{\Delta P_{wi_1}})(\Delta P_{wi_2}-\mu_{\Delta P_{wi_2}})\big]\\ \gamma^{(3)}_{\Delta P_{wi_1i_2i_3}}&=\beta^{(3)}_{\Delta P_{wi_1i_2i_3}}\\ &=E\big[(\Delta P_{wi_1}-\mu_{\Delta P_{wi_1}})(\Delta P_{wi_2}-\mu_{\Delta P_{wi_2}})\\ &\quad(\Delta P_{wi_3}-\mu_{\Delta P_{wi_3}})\big]\end{aligned} \tag{19}$$

where $\beta^{(n)}_{\Delta P_{wi_1\cdots i_n}}$ is the n^{th} order cross central moment and $\mu_{\Delta P_{wi_n}}$ is the mean of ΔP_{wi_n}. The expected values in (19) can be calculated directly when each wind power variation sample series is obtained. Hence by using (18) and (19), first three order cross cumulants of $\Delta\xi_k$ are obtained.

C. Modification of (14)

Firstly, a vector of the approximate values of ξ_k is calculated to be

$$\left[\xi_k\right]_{N_s\times 1} = \left[\xi_{k0}\right]_{N_s\times 1} + \sum_{i=1}^{m}\left\{\left[\mathrm{Re}(\frac{\partial\lambda_k}{\partial P_{wi}})\right]\left[\Delta P_{wi}\right]_{N_s\times 1}\right\} \tag{20}$$

where $\left[\xi_{k0}\right]_{N_s\times 1}$ is a vector with all the samples equal to the deterministic value ξ_{k0}. Then the maximums and minimums of the vector $\left[\xi_k\right]_{N_s\times 1}$ are determined. It is noted that there are possibilities that multiple maximums and multiple minimums exist in some cases. All the wind power data sets corresponding to the maximums and minimums of $\left[\xi_k\right]_{N_s\times 1}$ are recorded (each wind power data set $\left[P_{w1}, P_{w2}, \cdots P_{wm}\right]_{1\times m}$ is consist of m wind power data which are respectively from the same row of each $\left[P_{wi}\right]_{N_s\times 1}$ as the maximum or minimum in $\left[\xi_k\right]_{N_s\times 1}$).

Secondly, the deterministic eigenvalue analysis is carried out to compute ξ_k by using the recorded wind power data sets as output power of m wind power sources. ξ_{kl} and ξ_{kr} are the smallest and largest ξ_k in the deterministic eigenvalue analysis respectively. The probabilistic density of ξ_{kl} and ξ_{kr} are calculated by

$$\begin{array}{ll}\frac{N_{\xi_{kl}}}{N_s}\delta(x-\xi_{kl}), & \text{for} \quad x=\xi_{kl}\\ \frac{N_{\xi_{kr}}}{N_s}\delta(x-\xi_{kr}), & \text{for} \quad x=\xi_{kr}\end{array} \tag{21}$$

where $N_{\xi_{kl}}$ and $N_{\xi_{kr}}$ are the repeated numbers of ξ_{kl} and ξ_{kr} in the deterministic eigenvalue analysis respectively. Hence, the PDF and CDF of ξ_k with modified left and right ends are obtained. The form of PDF and CDF of ξ_k is similar to (14), but the probabilistic density values at left and right ends are changed as given by (21).

IV. Case Study

The probabilistic analysis of small-signal stability proposed in the previous sections is tested in a 16-machine 5-area power system with 3 grid-connected wind power sources, which is shown in Fig. 1. Since the selection of installing locations of the wind generators is not the issue of discussion in this paper, it is assumed that the wind farms have already been established at node 69, 70 and 71. This assumption does not affect the demonstration and test of the proposed method of probabilistic analysis.

The parameters of the wind generators and wind speed distributions for Case A, B and C below are given in Appendix B. The dynamic model of the DFIG rotor-side converter controller has been considered and also presented in Appendix B, as it is noted that the dynamics of rotor-side converter controller has more significant impact on the power system small-signal stability than grid-side converter controller in [1]-[6]. The network data, system load condition, synchronous generator model and parameters are given by [29]. Since the paper mainly focuses on the impact of wind farms on the power system small-signal stability, a simple one-order excitation system has been employed for all the synchronous generators (Appendix C) and there is no PSS installed.

A. Analytical Method and Monte Carlo Simulation

1) Case A (Normal load level without correlations of wind power sources): From the deterministic small-signal stability analysis, the 29^{th} eigenvalue is identified to be the critical oscillation mode, i.e., $\lambda_{29} = -0.0106 \pm j3.3004$. Hence deterministically the system is stable. The wind farm at node 69, 70 and 71 is denoted to be the 1^{st}, 2^{nd} and 3^{rd} source of wind generation respectively. The sensitivity computation of the critical eigenvalue with respect to three sources of wind generation is

$$\frac{\partial\lambda_{29}}{\partial P_{w1}} = 0.0096 - j0.0489, \frac{\partial\lambda_{29}}{\partial P_{w2}} = 0.0083 - j0.0466$$
$$\frac{\partial\lambda_{29}}{\partial P_{w3}} = 0.0075 - j0.0394$$

Table I shows the first five orders of moments and cumulants of three wind power variations computed by using (3) and (4). Table II gives the first five orders of cumulants and the central moments of the real part of the critical eigenvalue obtained from (8) and (9). Table III gives the first six coefficients of the Gram-Charlier expansion. Then the probabilistic distributions of the standardized critical eigenvalue are computed by use of (10) and (11) and the PDF of the critical eigenvalue is calculated by using (12) and (13). Finally, the PDF curve obtained is modified by using (14) as presented in details in the following. By deterministic eigenvalue analysis, ξ_{29l} and ξ_{29r} are calculated to be -0.0185 and 0.0094 when all the wind generation sources are at the cut-in wind power (0p.u.) and the furling wind power (1p.u.) respectively. According to the CDF of wind speed $F_{si}(\cdot)$, the probabilistic density values at ξ_{29l} and ξ_{29r} are computed to be $0.0117\delta(x+0.0185)$ and $0.0003\delta(x-0.0094)$ respectively. Hence, the modified PDF curve of the real part of the critical eigenvalue is obtained in Fig. 2 according to (14).

TABLE I
Moments and Cumulants of Three Wind Power Variations

Moments of Three Wind Power Variations				
$\alpha^{(1)}_{\Delta P_{wi}}$*	$\alpha^{(2)}_{\Delta P_{wi}}$	$\alpha^{(3)}_{\Delta P_{wi}}$	$\alpha^{(4)}_{\Delta P_{wi}}$	$\alpha^{(5)}_{\Delta P_{wi}}$
0.0319	0.1080	0.0281	0.0262	0.0126
Cumulants of Three Wind Power Variations				
$\gamma^{(1)}_{\Delta P_{wi}}$	$\gamma^{(2)}_{\Delta P_{wi}}$	$\gamma^{(3)}_{\Delta P_{wi}}$	$\gamma^{(4)}_{\Delta P_{wi}}$	$\gamma^{(5)}_{\Delta P_{wi}}$
0.0319	0.1070	0.0178	−0.0111	−0.0104

* $i = 1, 2, 3$ in this case.

It is well known that the convergence of Gram-Charlier expansion varies from different conditions and there is no theoretical simple way to determine the convergent order for Gram-Charlier expansion. The convergent order of the series is usually determined by trial and observation [17]. The Gram-Charlier expansion with different orders is tried extensively for applying the probabilistic small-signal stability analysis

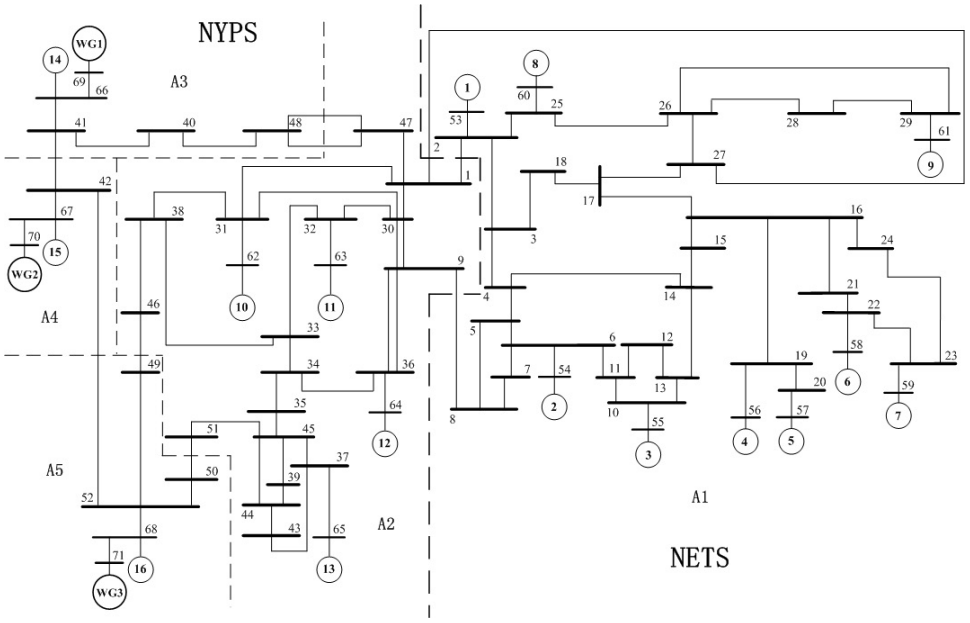

Fig. 1. Line diagram of example 16-machine 5-area power system integrated with wind power generation.

TABLE II
CUMULANTS AND CENTRAL MOMENTS OF CRITICAL EIGENVALUE VARIATION

Cumulants of Critical Eigenvalue Variation (Real Part)				
Mean	Variance*	$\gamma^{(3)}_{\Delta\xi_{29}}$	$\gamma^{(4)}_{\Delta\xi_{29}}$	$\gamma^{(5)}_{\Delta\xi_{29}}$
8.10×10^{-4}	2.32×10^{-5}	3.35×10^{-8}	-1.82×10^{-10}	-1.51×10^{-12}
Central Moments of Critical Eigenvalue Variation (Real Part)				
$\beta^{(1)}_{\Delta\xi_{29}}$	$\beta^{(2)}_{\Delta\xi_{29}}$	$\beta^{(3)}_{\Delta\xi_{29}}$	$\beta^{(4)}_{\Delta\xi_{29}}$	$\beta^{(5)}_{\Delta\xi_{29}}$
0	2.32×10^{-5}	3.35×10^{-8}	1.14×10^{-9}	6.26×10^{-12}

* The variance of $\Delta\xi_k$ is equal to $\gamma^{(2)}_{\Delta\xi_k}$.

TABLE III
COEFFICIENTS OF GRAM-CHARLIER EXPANSION (REAL PART)

g_0	g_1	g_3	g_4	g_5	g_6
1	0	0	−0.2989	−0.3382	0.5794

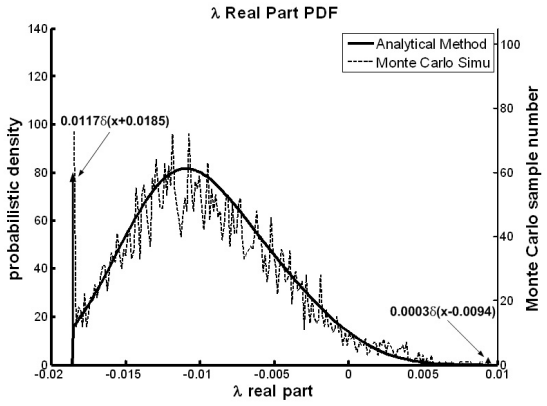

Fig. 2. Real part PDF of critical eigenvalue obtained by analytical method and Monte Carlo simulation (Case A).

proposed in this paper. It has been observed that the proposed method with first five orders can achieve sufficient accuracy to approximate the probabilistic density curve from the result of Monte Carlo simulation (with 5000 iterations) shown in Fig. 2.

A comparison of computation time between the Monte Carlo simulation and the analytical method proposed has been carried out. Based on the same computational resource (Dell OptiPlex 745, Intel Core 2 CPUs 2.66GHz, 3GB RAM), the time of the Monte Carlo simulation with 5000 iterations is 15236.48 seconds, while only 38.56 seconds for the analytical method with first five-order Gram-Charlier expansion is needed. The analytical method is about 395 times faster than the Monte Carlo simulation.

According to the PDF of Fig. 2 it can be obtained that

$$P(\xi_{29} < 0) = \int_{-\infty}^{0} f_{\xi_{29}}(x)dx = 0.9710 \qquad (22)$$

Eq. (22) indicates that when the stochastic variation of wind generation is considered, the critical eigenvalue of the example power system has a probability of 97.10% to remain in the left half-plane. Hence although the system is considered to be stable by the deterministic analysis, as the critical eigenvalue is $\lambda_{29} = -0.0106 \pm j3.3004$, it still has a probability of 2.90% to be unstable due to the uncertainty of wind generation.

2) Case B (Load level close to the static stability limit without correlations of wind power sources): At a stressed load condition, the 29^{th} eigenvalue is still identified to be the critical oscillation mode, $\lambda_{29} = -0.0005 \pm j3.2445$. Hence deterministically the system is stable but very close to the static stability limit. The sensitivity computation of the critical eigenvalue with respect to three sources of wind generation is

$$\frac{\partial \lambda_{29}}{\partial P_{w1}} = 0.0116 - j0.0614, \frac{\partial \lambda_{29}}{\partial P_{w2}} = 0.0100 - j0.0589$$
$$\frac{\partial \lambda_{29}}{\partial P_{w3}} = 0.0085 - j0.0516$$

By employing the same procedure as in Case A, the PDF curve of the real part of the critical eigenvalue is shown by Fig. 3. Fig. 3 also displays the confirmation from the result of Monte Carlo simulation (with 5000 iterations).

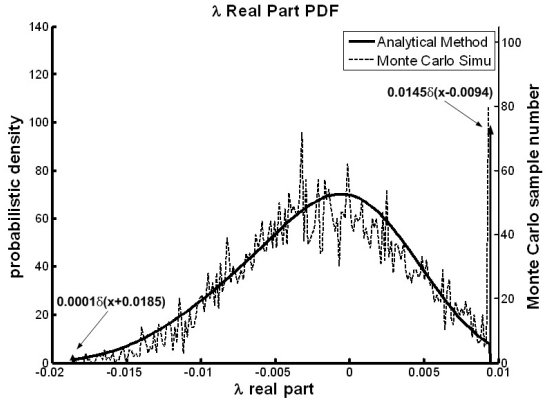

Fig. 3. Real part PDF of critical eigenvalue obtained by analytical method and Monte Carlo simulation (Case B).

According to the PDF of Fig. 3 it can be obtained that

$$P(\xi_{29} < 0) = \int_{-\infty}^{0} f_{\xi_{29}}(x)dx = 0.6112 \qquad (23)$$

Eq. (23) indicates that in the case of the stressed load level of the example system close to the static stability limit, the probability of the critical eigenvalue remaining in the left half-plane drops dramatically to 61.12%. Hence the system could become unstable with a high possibility when the stochastic variation of wind generation is considered.

3) Case C (Normal load level with certain correlations of wind power sources): In this case, the correlations between three wind power sources are taken into account and the load condition of Case A is selected. Hence, the results of deterministic small-signal stability analysis and sensitivity computation are exactly the same as Case A. Since there is no wind speed data available for the example system, the correlation coefficient matrix $\left[\rho_{ij}\right]_{3\times 3}$ is assumed according to the geographical distance between the three wind farms given by

$$\left[\rho_{ij}\right]_{3\times 3} = \begin{bmatrix} 1 & 0.8 & 0 \\ 0.8 & 1 & 0 \\ 0 & 0 & 1 \end{bmatrix} \qquad (24)$$

Eq. (24) suggests that the first two wind power sources are strongly correlated, while the third is independent with the other two due to the long distance. By employing the procedure presented in Section III, the 2^{nd} and 3^{rd} order cross cumulants of $\Delta\xi_{29}$ are computed by (18) to be

$$\gamma^{(2)}_{\Delta\xi_{29}} = 3.63 \times 10^{-5}, \gamma^{(3)}_{\Delta\xi_{29}} = 9.02 \times 10^{-8}$$

The probabilistic density of ξ_{29l} and ξ_{29r} is calculated by (21) to be

$$\frac{N_{\xi_{29l}}}{N_s}\delta(x - \xi_{29l}) = 0.0396\delta(x + 0.0185)$$
$$\frac{N_{\xi_{29r}}}{N_s}\delta(x - \xi_{29r}) = 0.0028\delta(x - 0.0094)$$

Finally, the PDF curve of the real part of the critical eigenvalue is shown by Fig. 4. The result of Monte Carlo simulation (with 5000 iterations) in Fig. 4 has verified the proposed method when the correlations of wind power sources are considered.

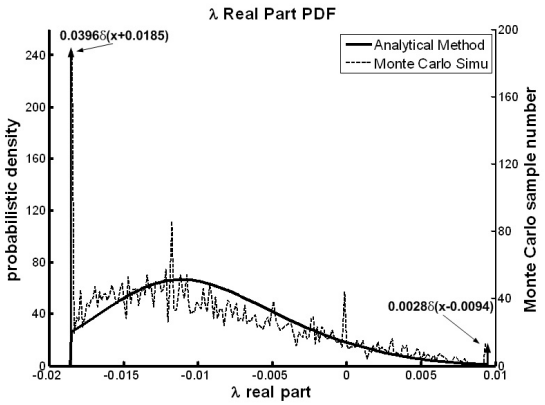

Fig. 4. Real part PDF of critical eigenvalue obtained by analytical method and Monte Carlo simulation (Case C).

According to the PDF of Fig. 4 it can be obtained that

$$P(\xi_{29} < 0) = \int_{-\infty}^{0} f_{\xi_{29}}(x)dx = 0.9334 \qquad (25)$$

Eq. (25) indicates that the consideration of correlation has changed the probability of system small-signal stability. However, the correlation has much less impact on the probabilistic stability than the varying load conditions as compared with Case B.

B. Probabilistic Analysis on Different Levels of Wind Penetration

Since the wind mean speed may vary from time to time, levels of wind penetration are variable and the operation point and load conditions of the power system may change, which can bring about the different probabilistic stability. Hence proposed probabilistic analysis is carried out for the example power system with changing level of wind generation. Fig. 5 shows the result of computation of the probability of small-signal stability of the example power system when $P_{wi0}, (i = 1, 2, 3)$ varies from 0 to 1 per unit unanimously. Obviously it can be seen that with the increase of level of wind penetration to the example power system, the probability of small-signal stability of the system decreases. The worst case is that when three wind farms operate at their rated generation capacity, and the system is only of a probability of just above 20% to be stable.

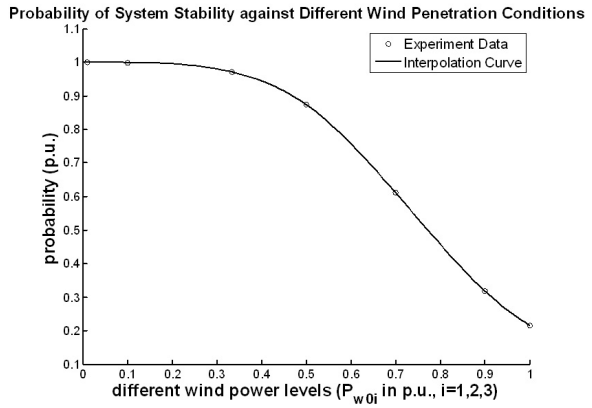

Fig. 5. Probability of system stability against different wind penetration conditions.

V. Conclusion

The paper presents a method of probabilistic analysis of power system small-signal stability considering the stochastic uncertainty introduced from multiple grid-connected sources of wind generation. The spatial correlations of different grid-connected wind farms are considered. The method can directly determine the system probabilistic stability by performing just once the proposed step-by-step probabilistic analysis. Hence it is very computationally efficient especially when applied in large-scale power systems, as compared to the non-analytical method of Monte Carlo simulation.

In the paper, an example 16-machine power system with 3 grid-connected wind farms is presented. The correctness and accuracy of the proposed analytical method are confirmed by the results of Monte Carlo simulation. The example shows that though the system is stable deterministically, there exists the certain probability that the system can lose stability due to the stochastic fluctuations caused by wind generation. With increasing level of wind penetration, the probability of instability could grow accordingly, threatening the stable operation of the power system.

Appendix A
The n^{th} Order Moment Derivation of ΔP_{wi}

$$\alpha^{(n)}_{\Delta P_{wi}} = \int_{-P_{w0i}}^{P_{ri}-P_{w0i}} x^n dF_{pi}(x) = \int_{-P_{w0i}}^{P_{ri}-P_{w0i}} x^n f_{pi}(x)dx$$
$$= \int_{-P_{w0i}}^{-P_{w0i}} x^n[1-(F_{si}(v_{fi})-F_{si}(v_{ci}))]\delta(x+P_{w0i})dx$$
$$+ \int_{-P_{w0i}}^{P_{ri}-P_{w0i}} x^n \frac{b_i}{d_i}\Big(\frac{x-h_i+P_{w0i}}{d_i}\Big)^{b_i-1} e^{\left[-\left(\frac{x-h_i+P_{w0i}}{d_i}\right)^{b_i}\right]}dx$$
$$+ \int_{P_{ri}-P_{w0i}}^{P_{ri}-P_{w0i}} x^n[F_{si}(v_{fi})-F_{si}(v_{ri})]\delta\big[x-(P_{ri}-P_{w0i})\big]dx$$
$$= \big[1-(F_{si}(v_{fi})-F_{si}(v_{ci}))\big](-P_{w0i})^n$$
$$+ \big[F_{si}(v_{fi})-F_{si}(v_{ri})\big](P_{ri}-P_{w0i})^n$$
$$+ \int_{-P_{w0i}}^{P_{ri}-P_{w0i}} x^n \frac{b_i}{d_i}\Big(\frac{x-h_i+P_{w0i}}{d_i}\Big)^{b_i-1} e^{\left[-\left(\frac{x-h_i+P_{w0i}}{d_i}\right)^{b_i}\right]}dx$$

By performing the variable transformation twice, i.e., $t = x - h_i + P_{w0i}$ and $\tau = (\frac{t}{d_i})^{b_i}$, the above equation becomes

$$\begin{aligned}\alpha^{(n)}_{\Delta P_{wi}} &= \big[1-(F_{si}(v_{fi})-F_{si}(v_{ci}))\big](-P_{w0i})^n \\ &+ \big[F_{si}(v_{fi})-F_{si}(v_{ri})\big](P_{ri}-P_{w0i})^n \\ &+ \int_{(-\frac{h_i}{d_i})^{b_i}}^{(\frac{P_{ri}-h_i}{d_i})^{b_i}} \Big[d_i\tau^{\frac{1}{b_i}}+(h_i-P_{w0i})\Big]^n e^{-\tau}d\tau \\ &= \big[1-(F_{si}(v_{fi})-F_{si}(v_{ci}))\big](-P_{w0i})^n \\ &+ \big[F_{si}(v_{fi})-F_{si}(v_{ri})\big](P_{ri}-P_{w0i})^n \\ &+ \sum_{k=0}^{n} C_n^k (d_i)^k (h_i-P_{w0i})^{n-k} \int_{(-\frac{h_i}{d_i})^{b_i}}^{(\frac{P_{ri}-h_i}{d_i})^{b_i}} \tau^{\frac{k}{b_i}} e^{-\tau}d\tau\end{aligned} \quad (26)$$

Appendix B
Wind Power Generator Model and Distribution Parameters

A 70MW DFIG model in [34] is used for all three wind farms and the parameters in p.u. are

$$H = 1.7\text{s}, D = 0.0, X_s = 2.9, X_r = 2.9, X_m = 2.6, R_s = 0.0,$$
$$R_r = 0.0013, P_{w0} = 0.3333(\text{Case A and C}), 0.7000(\text{Case B})$$

The DFIG rotor-side converter controller model used in the example system is shown by Fig. 6, where $K_P = 30, K_Q = 30$.

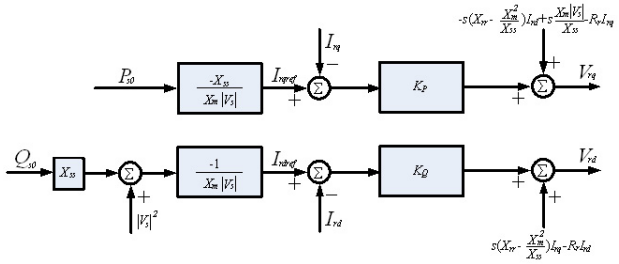

Fig. 6. The DFIG rotor-side converter control model.

The parameters of the wind speed distribution are [25]

$$v_c = 4\text{m/s}, v_r = 10\text{m/s}, v_f = 22\text{m/s}, P_r = 1.0\text{p.u.},$$
$$\mu = 6\text{m/s(Case A and C)}, 8.2\text{m/s(Case B)}, \sigma = 2.5$$

Appendix C
Excitation System Model of Synchronous Generators and its Parameters

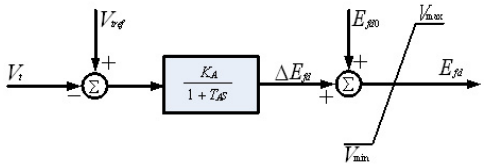

Fig. 7. The excitation system model of synchronous generators.

$$K_A = 7.4, T_A = 0.1s, V_{\max} = 10.0, V_{\min} = -10.0$$

ACKNOWLEDGMENT

The authors would like to acknowledge the support of the EPSRC UK-China joint research consortium (EP/F061242/1), the science bridge award (EP/G042594/1), UK, Jiangsu Power Company, China, and the Chinese Scholarship Council, the Fund of Best Post-Graduate Students of Southeast University, China. Prof. Haifeng Wang is a member of the international innovation team of superconducting technology for electrical engineering at the Institute of Electrical Engineering, Beijing, China, sponsored by the Chinese Academy of Sciences, China.

REFERENCES

[1] J. G. Slootweg and W. L. Kling, "The Impact of Large Scale Wind Power Generation on Power System Oscillations," *Electric Power Systems Research*, vol. 67, pp. 9-20, June, 2003.

[2] F. Mei and B. C. Pal, "Modeling of the Doubly-fed Induction Generator for Power System Stability Study,"*IEEE Power Engineering Society General Meeting*, 2008.

[3] J. J. Sanchez-Gasca, N. W. Miller, W. W. Price, "A Modal Analysis of a Two-Area System with Significant Wind Power Penetration," *Power Systems Conference and Exposition*, 2004.

[4] A. Mendonca, and J. A. Pecas Lopes, "Impact of Large Scale Wind Power Integration on Small Signal Stability," *Future Power Systems*, pp. 1-5, 2005.

[5] D. Gautam, V. Vittal, "Impact of DFIG Based Wind Turbine Generators on Transient and Small Signal Stability of Power Systems," *Power and Energy Society General Meeting*, pp. 1-6, 2009.

[6] E. N. Hinrichsen, P. J. Nolan, "Dynamics and Stability of Wind Turbine Generators," *IEEE Trans. on Power Apparatus and Systems*, vol. PAS-101, 1982.

[7] B. Borkowska, "Probabilistic Load Flow," *IEEE Trans. on Power Apparatus and Systems*, vol. PAS-93, pp. 752-759, 1974.

[8] R. N. Allan, B. Borkowska,and C. H. Grigg, "Probabilistic analysis of power flows," *Proc. Inst. Elect. Eng. (London)*, vol. 121, pp. 1551-1556, Dec. 1974.

[9] R. N. Allan and M. R. G. Al-Shakarchi, "Probabilistic a.c. load flow," *Proc. Inst. Elect. Eng. 123*, no. 6, pp. 531-536, 1976.

[10] R. C. Burchett and G. T. Heydt, "Probabilistic Methods For Power System Dynamic Stability Studies," *IEEE Trans. on Power Apparatus and Systems*, vol. PAS-97, pp. 695-702, 1978.

[11] R. C. Burchett and G. T. Heydt, "A generalized method for stochastic analysis of the dynamic stability of electric power system," *IEEE PES SM Paper*, A78528, 1978.

[12] H. Q. Yi, Y. H. Hou, S. J. Cheng, H. Zhou and G. G. Chen, "Power system probabilistic small signal stability analysis using two point estimation method," *UPEC*, 2007.

[13] C. K. Pang, Z. Y. Dong, P. Zhang and X. Yin, "Probabilistic Analysis of Power System Small Signal Stability Region," *International Conference on Control and Automation*, June, 2005.

[14] K. W. Wang, C. T. Tse and K. M. Tsang, "Algorithm for Power System Dynamic Stability Studies Taking Account the Variation of Load Power," *4th International Conference on Advances in Power System Control, Operation and Management*, Nov., 1997.

[15] C. Y. Chung, K. W. Wang, C. T. Tse, X. Y. Bian and A. K. David, "Probabilistic Eigenvalue Sensitivity Analysis and PSS Design in Multimachine Systems," *IEEE Trans. on Power Systems*, vol. 18, pp. 1439-1445, 2003.

[16] X. Y. Bian, C. T. Tse, K. W. Wang and C. Y. Chung, "Probabilistic design of FACTS device for power system small signal stability enhancement," *18th International Conference on Electricity Distribution*, June, 2005.

[17] P. Zhang and S. T. Lee, "Probabilistic load flow computation using the method of combined cumulants and Gram-Charlier expansion," *IEEE Trans. on Power Systems*, vol. 19, pp. 676-682, 2004.

[18] Z. Hu and X. F. Wang, "A Probabilistic Load Flow Method Considering Branch Outages," *IEEE Trans. on Power Systems*, vol. 21, pp. 507-514, 2006.

[19] Y. Y. Hong and Y. F. Luo, "Optimal VAR Control Considering Wind Farms Using Probabilistic Load-Flow and Gray-Based Genetic Algorithms," *IEEE Trans. on Power Delivery*, vol. 24, pp. 1441-1449, 2009.

[20] A. Schellenberg, W. Rosehart and J. Aguado, "Cumulant-Based Probabilistic Optimal Power Flow (P-OPF) with Gaussian and Gamma Distributions," *IEEE Trans. on Power Systems*, vol. 20, pp. 773-781, 2005.

[21] A. Schellenberg, W. Rosehart and J. Aguado, "Cumulant-Based Stochastic Optimal Power Flow (S-OPF) for Variance Optimization," *IEEE PES SM Paper*, vol. 1, pp. 473-478, 2005.

[22] K. W. Wang, C. Y. Chung, C. T. Tse and K. M. Tsang, "Improved probabilistic method for power system dynamic stability studies," *IEE Proc. Gener. Transm. Distrib.*, vol. 147, Jan., 2000.

[23] Z. Xu, Z. Y. Dong and P. Zhang, "Probabilistic Small Signal Analysis using Monte Carlo Simulation," *IEEE PES SM Paper*, 1489425, 2005.

[24] C. Wang, L. B. Shi, L. Z. Yao, L. M. Wang, Y. X. Ni and M. Bazargan, "Modelling Analysis in Power System Small Signal Stability Considering Uncertainty of Wind Generation," *IEEE PES SM Paper*, 5589646, 2010.

[25] I. Abouzahr and R. Ramakumar, "An approach to assess the performance of utility-interactive wind electric conversion systems," *IEEE Trans. on Energy Conversion*, vol. 6, pp. 627-638, 1991.

[26] M. Kendall, *Kendall's Advanced Theory Statisitcs*. New York (NY, USA): Oxford Univeristy Press, 1987.

[27] H. Cramer, *Numerical Methods of Statistics*. Princeton, NJ: Princeton University Press, 1946.

[28] Z. Y. Dong, C. K. Pang and P. Zhang, "Power System Sensitivity Analysis for Probabilistic Small Signal Stability Assessment in a Deregulated Environment," *International Journal of Control, Automation and Systems*, vol. 3, pp. 355-362, June, 2005.

[29] G. Rogers, *Power System Oscillations*. Kluwer Academic Publishers, 2000.

[30] L. Freris and D. Infield, *Renewable energy in power systems*. John Wiley and Sons, 2008.

[31] Julio Usaola, "Probabilistic load flow with correlated wind power injections," *Electric Power Systems Research*, 2010.

[32] J. M. Morales, L. Baringo, A. J. Conejo and R. Minguez, "Probabilistic power flow with correlated wind sources," *IET Gener. Transm. Distrib.*, vol. 4, 2010.

[33] G. Papaefthymiou and D. Kurowicka, "Using Copulas for Modeling Stochastic Dependence in Power System Uncertainty Analysis," *IEEE Trans. on Power Systems*, vol. 24, 2009.

[34] H. Akagi and H. Sato, "Control and Performance of a Doubly-Fed Induction Machine Intended for a Flywheel Energy Storage System," *IEEE Trans. on Power Electronics*, vol. 17, pp. 109-116, 2002.

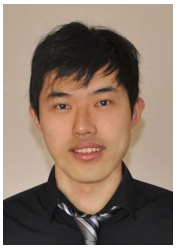

S. Q. Bu (S'11) received the B.S. and M.S. from school of electrical engineering, Southeast University, China, in 2006 and 2008 respectively. Currently, he is a PhD student in the electric power and energy research cluster, the Queens University of Belfast, UK. His research interests are power system stability analysis and operation control, including wind power generation, PEV and HVDC technology. His contact e-mail address is sbu01@qub.ac.uk.

W. Du (corresponding author) is working as a Research Fellow at the Queens University of Belfast. Her main research interests are power system stability analysis and control, including energy storage systems, FACTS, EV and renewable power generation. Her contact e-mail address is ddwenjuan@qub.ac.uk.